

## Microwave Radiation from Slant Cut Cylindrical Antennas – Modeling an Experiment

C. Vollaire, L. Nicolas

CEGELY - UPRESA CNRS 5005, BP 163 - 69131 Ecully Cedex - France

K. A. Connor, S. J. Salon

Rensselaer Polytechnic Institute, Troy, NY 12180-3590 - USA

B. G. Ruth, L. F. Libelo

Army Research Laboratory, Adelphi, MD 20783-1197 - USA

**Abstract**—A series of Vlasov-type high power microwave launchers were investigated with several slant-cut angles. Finite element analysis using parallel computation was performed on a cluster of workstations and compared with low-power measurements made on a variety of such antennas. Good agreement between the main features of the radiation patterns were observed. However, not all details were reproduced.

**Index terms**—Microwave antennas, Finite element methods, Parallel algorithms, Distributed memory systems.

### I. INTRODUCTION

We have been investigating the use of simple Vlasov-type launching structures for high-power microwave applications [1]. It is the eventual goal of this work to permit a high-power beam to be launched from an array of such radiators. Electromagnetic field information is obtained in three dimensions with a Finite Element (FE) model that uses the Engquist-Majda Absorbing Boundary Conditions (ABC) [2]. We have previously compared this analysis to the field radiated by an electric dipole. Here we consider experimental data obtained with a variety of antenna configurations. We also analyzed this data using two dimensional FE analysis [3]. Somewhat surprisingly, we found that good qualitative understanding of these launcher geometries could be obtained in this manner, but none of details of the actual radiation patterns were reproduced.

Only parallel computation actually enables modeling such devices in three dimensions because it provides enough memory. That is why we have used a parallel distributed memory computer to model such geometries: 10 DEC ALPHA workstations linked with a FDDI ring and fitted with Parallel Virtual Machine (PVM) software. When three dimensional analysis is performed, the main features and nearly all of the power are properly accounted for.

The experimental launcher configurations are first described. The FE formulation for the near field computation is then given. Its implementation on a distributed memory parallel computer is presented. Computed radiation patterns concerning four different slant cut angle configurations are

finally compared to the measurements.

### II. EXPERIMENT

A very large variety of radiator configurations with different slant cut angles, windows materials, flares and many other modifications have been studied in the laboratory [4]. Here we consider four choices of angles  $\alpha$ :  $30^\circ$ ,  $45^\circ$ ,  $60^\circ$  and  $90^\circ$ . The experimental geometry is shown in Fig. 1.

Measurements were made for both horizontal and vertical rotation angles. For the data to be presented,  $\phi = 90^\circ$  is the symmetry plane of the radiator.

### III. MODELING

#### A. Formulation

We are dealing with frequency domain open boundary electromagnetic field problems. According to Maxwell's equations, the magnetic field  $\mathbf{H}$  and the electric field  $\mathbf{E}$  satisfy vector wave equations. The following analysis is made only for the  $\mathbf{H}$  field formulation. All the steps can be applied to the  $\mathbf{E}$  field formulation as well.

A penalty term, which makes the field divergence free, is added to the formulation to avoid spurious reflections [2]. 3D second order vector Engquist-Majda ABC are used to

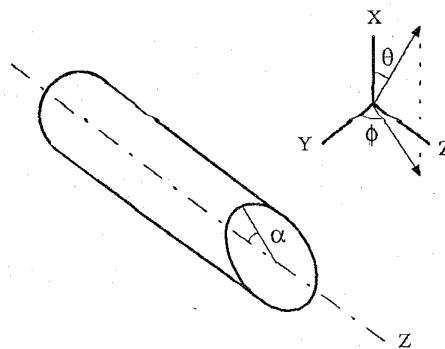


Fig. 1. Geometry of cylindrical launcher.  $\alpha$  is the slant cut angle.

Manuscript received November 3, 1997.

C. Vollaire, vollair@trotek.ec-lyon.fr; L. Nicolas, laurent@trotek.ec-lyon.fr, http://cegely.ec-lyon.fr; K.A.Connor, connor@rpi.edu.

truncate the 3D finite element region [2]. Outer surfaces are then rectangles, which saves mesh nodes for this cylindrical launcher geometry:

$$\mathbf{n} \times \nabla \times \mathbf{H} \cong g_{ABC}(\mathbf{H}) = j k_0 \mathbf{H}_t - \frac{j}{2k_0} \nabla_t^2 \mathbf{H}_t \quad (1)$$

Finally, the formulation for microwave problems in terms of magnetic fields is given by (2). Three types of surfaces are considered: external surfaces (*S<sub>ext</sub>*), perfect electric surfaces (*S<sub>spec</sub>*) and source surfaces (*S<sub>sour</sub>*). (The notation used is discussed in [2].)

$$\int_V \left[ (\nabla \mathbf{W} \times \frac{1}{\epsilon_r} \nabla \times \mathbf{H}) + \mathbf{W} k_0^2 \mu_r \mathbf{H} \right] dv - \int_V [(\nabla \mathbf{W})(\nabla \cdot \mathbf{H})] dv \quad (2)$$

$$+ \int_{S_{ext+Spec}} \mathbf{W} \mathbf{n} \cdot \nabla \cdot \mathbf{H} ds - \int_{S_{ext}} \mathbf{W} g_{ABC}(\mathbf{H}) ds = \int_{S_{sour}} \mathbf{W} \mathbf{J} ds$$

This formulation leads to 3 complex unknowns (6 degrees of freedom) per node. For such problems, the mesh size is related to the frequency of the source: 10 nodes per wavelength have to be used to obtain good accuracy. The distance between the device and outer boundary must be at least equal to 1 wavelength. These requirements lead to 50000 node meshes in order to model Vlasov-type launching structures in three dimensions (Table I). Only parallel computation provides access to enough memory to compute these geometries.

### B. Modeling the Source

The experimental antennas were driven with a source that produces a relatively clean  $TM_{01}$  mode, so that is the only mode used as a source for the FE analysis. Such an excitation is modeled by inserting a current sheet at a quarter wavelength from the bottom of the guide (fig. 2). The surface current density on this sheet is designed so that only the  $TM_{01}$  mode is excited [5].

### C. Far field computation

The far field radiated is computed by an integral approach.

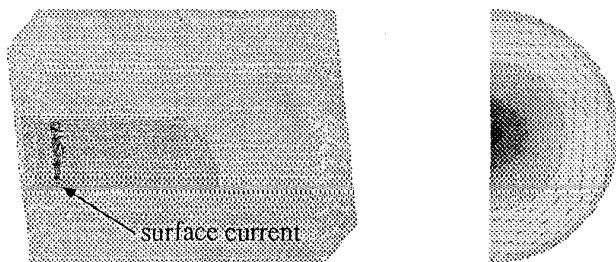


Fig. 2. Excitation of the launcher. Right: surface current density

By using the 3D FE solutions of the near field, fictitious electric and magnetic sources are first calculated on an equivalent surface surrounding the device. Plane wave approximations are then applied, and the far field is computed by surface integration [6]:

$$\mathbf{H}_{far} = \mathbf{H}_A + \mathbf{H}_F \quad \mathbf{E}_{far} = \mathbf{E}_A + \mathbf{E}_F \quad (3)$$

with

$$\mathbf{H}_F \approx -j\omega \mathbf{F} \quad (\mathbf{E}_F)_\theta = \eta(\mathbf{H}_F)_\phi \quad \text{and} \quad (\mathbf{E}_F)_\phi = -\eta(\mathbf{H}_F)_\theta \quad (4)$$

$$\mathbf{E}_A \approx -j\omega \mathbf{A} \quad \eta(\mathbf{H}_A)_\theta = -(\mathbf{E}_A)_\phi \quad \text{and} \quad \eta(\mathbf{H}_A)_\phi = (\mathbf{E}_A)_\theta$$

and the vector potentials are defined by:

$$\mathbf{A} = \frac{\mu}{4\pi} \iint_S \mathbf{n} \times \mathbf{H} \frac{e^{-j\beta R}}{R} ds \quad \mathbf{F} = -\frac{\epsilon}{4\pi} \iint_S \mathbf{n} \times \mathbf{E} \frac{e^{-j\beta R}}{R} ds \quad (5)$$

## IV. PARALLEL ALGORITHMS

### A. Assembling

The program is a Single Program Multi-Data type (SPMD) and the FE matrix is dispatched on every processor to optimize memory use. The global coefficients matrix is assembled by degrees of freedom [7-8]. This permits the three lines (three coordinates) corresponding to a node to be assembled simultaneously. Load balancing is nearly perfect because of the constant bandwidth of the global matrix and because no message passing is required. Due to this method, the speedup is optimal [8].

### B. Introduction of boundary conditions

Message passing is necessary to introduce the boundary conditions on the symmetry planes because a global modification of the matrix system is required. However, this step does not significantly affect the total CPU time.

### C. Symmetrization of the matrix system

The introduction of both ABC and a penalty function results in a non-symmetric system matrix. This is approximately symmetrized by adding it to its transposed matrix. This method has shown to give good results because the structure of the global matrix remains symmetric, the non-symmetry affects only some terms on the external surface and the ABC terms located on the diagonal are dominant [9]. This operation requires message passing too, but, as previously, it does not reduce global parallel performance.

### D. Solve the system of equations

A Conjugate Gradient (CG) with diagonal preconditioning method (DP) has been implemented. Because this method is iterative, small-scale parallelism is used. The

preconditioning matrix is computed by inverting the diagonal terms of the coefficients matrix. Preconditioning is obtained by a vector-vector multiplication which is performed in parallel. No message passing is required.

When using this type of preconditioning, a matrix-vector multiplication is required to compute the residual vector at each iteration. This multiplication is performed in parallel [8,10-13]: each processor computes a partial residual vector and broadcasts it to all the others. Hence, the concatenation is done in SPMD mode.

## V. RESULTS

The computations were performed on 8 processors of the cluster of workstations. Four configurations were analyzed. Table 1 shows the number of nodes, the number of first hexahedral elements and the number of iterations needed to solve the matrix system. The CPU time per processor required to compute the entire problem is also given.

Following Vlasov's quasi-optical analysis, the slant-cut angle should correspond to the direction of propagation of the  $TM_{01}$  mode propagating in the cylindrical waveguide:  $\tan^{-1}(k_r/k_z)$ . Thus, the four cases considered range from a simple cylindrical pipe cut straight ( $\alpha=90^\circ$ ), for which a variety of analytic field solutions are available, to angles that bracket the optimum launch angle for the frequency and guide dimensions used (approximately  $34^\circ$ ).

Fig. 3 shows the problem mesh for a  $60^\circ$  slant cut angle geometry. Fig. 4 shows the near magnetic field pattern generated for the case of a  $TM_{01}$  mode in the XZ plane at the instant  $t = 0^\circ$ . The operating frequency is 8.6 GHz and the radius of the guide is 23.8 mm.

## VI. DISCUSSION

For each of the cases depicted in fig. 5 - 8, the solid lines are the experimental data, while the filled circles are the numerically determined values. The peak experimental and numerical fields do indeed occur near the mode propagation direction for each choice of  $\alpha$  and the bulk of the radiated power also falls in the same angle range. Note that the maximum difference between the largest and the smallest features of the radiation pattern occurs near the quasi-optical design angle. However, cutting the angle even more obliquely (smaller  $\alpha$ ) produces an even larger difference and, thus, a tighter beam.

TABLE I  
CPU TIME PER PROCESSOR AND NUMBER OF ITERATIONS FOR THE  
RESOLUTION OF THE FOUR CASES WITH THE DP.

	nodes	elements	iterations	time/processor (s)
$\alpha = 90^\circ$	55575	50816	2428	37511
$\alpha = 60^\circ$	62415	57168	2931	48474
$\alpha = 45^\circ$	45084	40810	5487	55296
$\alpha = 30^\circ$	54332	49290	6603	49290

There are several differences between the numerical and experimental approaches that can account for the differences between the two results. First, is the assumption of perfect conductivity for the launcher material, as noted above. Second, only one mesh element is used to represent the cut end of the launcher in the FE analysis. Third, none of the mounting structures and feeds for the experimental antenna are included in the numerical model.

## VII. CONCLUSION

In this paper, a series of Vlasov-type high power microwave launchers has been investigated with several slant-cut angles. Because of the large number of degrees of freedom required to model these geometries, the FE analysis has been performed using parallel computation. Results have been compared with low-power measurements made on a variety of such antennas. Good agreement between the main features of the radiation patterns was observed. However, several differences between the numerical and experimental approaches have been observed. Efforts are underway to address the issues cited in the previous section, but the overall quality of the results is sufficient for launcher design.

## REFERENCES

- [1] S. N. Vlasov, I. M. Orlova, "Quasi-optical transformer which transforms the waves in a circular waveguide to a highly directional beam of waves," *Radiophysics Quantum Electronics*, pp. 148-154, 1974.
- [2] L. Nicolas, K. A. Connor, S. J. Salon, B. G. Ruth, and L. F. Libelo, "Three dimensional FE analysis of high power microwave devices," *IEEE Trans. Magnetics*, pp. 1642-1645, March 1993.
- [3] L. Nicolas, K. A. Connor, S. J. Salon, B. G. Ruth, and L. F. Libelo, "Numerical and experimental studies of quasi-optical high power microwave launchers," *Int. J. IR and MM Waves*, 1991.
- [4] B. G. Ruth, C. D. R. Schelesiger, R. K. Dahlstrom, "Antenna measurements on the radiation component of an X-Band Vlasov-type mode convertor," *Int. J. IR and MM Waves*, pp. 869-878, 1989.
- [5] D.M. Pozar, *Microwave Engineering*, Addison-Wesley Publishing Company, 1990.
- [6] L. Nicolas, "An Integral-type approach for the computation of the far field radiated by microwave devices," *IEEE Trans. Magnetics*, pp. 3124-3127, September 1994.
- [7] D. Zois, "Parallel processing techniques for FE analysis: stiffnesses, loads and stresses evaluation," *Comp. and Struct.*, vol. 34, pp. 353-374, 1990.
- [8] C. Vollaire, L. Nicolas, and A. Nicolas, "Finite elements coupled with absorbing boundary conditions on parallel distributed memory computer," *IEEE Trans. Magnetics*, vol. 33, pp. 1448-1451, March 1997.
- [9] J. L. Yao Bi, "Methode des elements finis mixte et conditions aux limites absorbants pour la modelisation des phenomenes electromagnetiques hyperfrequences," Ecole Centrale de Lyon, ECL95-04, 1995.
- [10] Y. Saad, "Krylov subspace method on supercomputers," *SIAM J. Sci. Stat. Comput.*, vol. 10, pp. 1200-1232, November 1989.
- [11] K. Iwano, V. Cungoski, K. Keneda, H. Yamashita, "A parallel processing method in FE analysis using domain division," *IEEE Trans. Magnetics*, vol. 30, pp. 3598-3601, September 1994.
- [12] R. Lee, V. Chupongstimm, "A partitioning technique for finite element solution of electromagnetic scattering from electrically large dielectric cylinders," *IEEE Trans. Antenna Propagat.*, vol. 42, pp. 737-741, May 1994.
- [13] C. Vollaire, L. Nicolas, "Parallel iterative solvers for large sparse linear system of equations on a distributed memory computer," *Digest of COMPUMAG 97*, 1997.

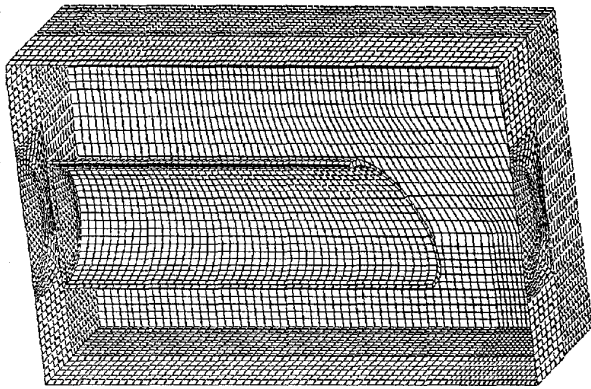


Fig. 3. Mesh of the problem (60° slant cut geometry)

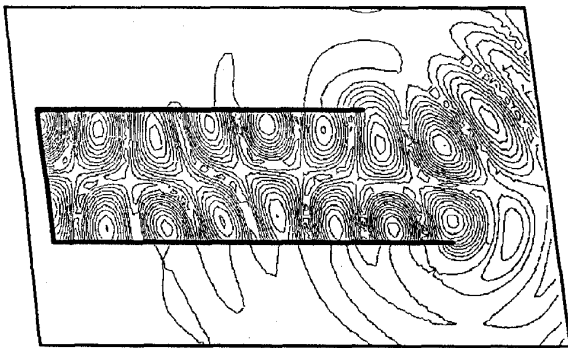


Fig. 4. Near magnetic field (60° slant cut geometry) -  $TM_{01}$  mode - results in the XZ plane - instant  $t = 0^\circ$

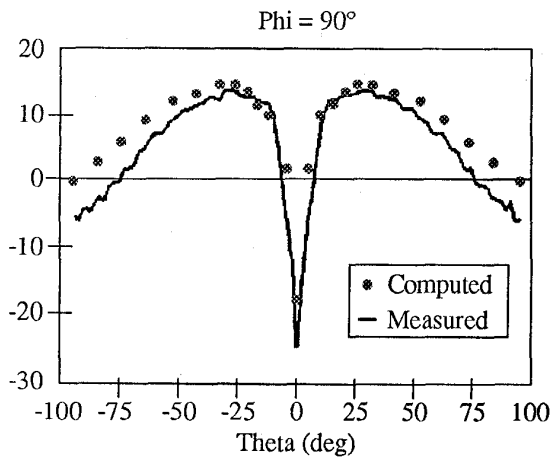


Fig. 5. Radiation pattern from a straight-cut cylindrical launcher ( $\alpha = 90^\circ$ )

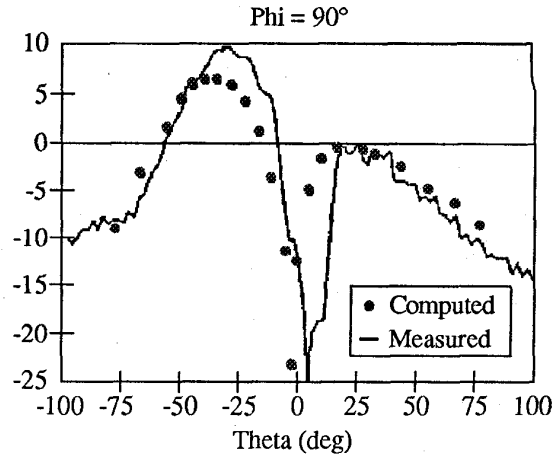


Fig. 6. Radiation pattern from a 60° slant-cut cylindrical launcher

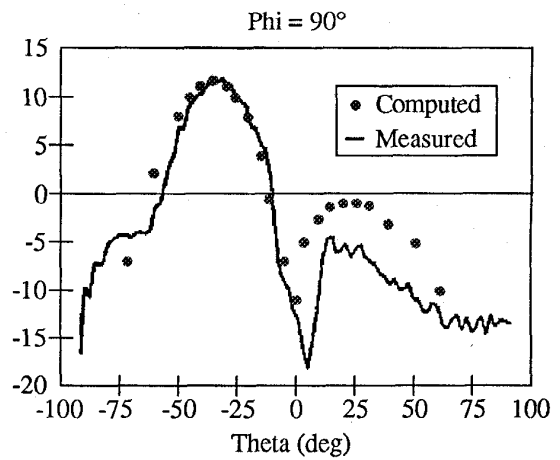


Fig. 7. Radiation pattern from a 45° slant-cut cylindrical launcher

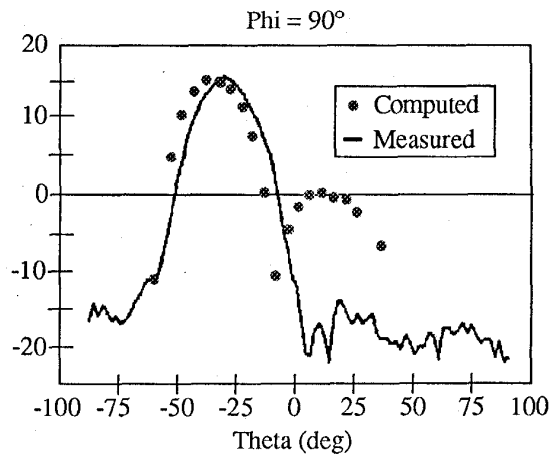


Fig. 8. Radiation pattern from a 30° slant-cut cylindrical launcher